

New Insights into the Lewis Acidity of Bis(hexafluoroacetylacetonato)copper(II) from EPR and Calorimetry Studies

David R. McMillin,^{1a} Russell S. Drago,^{*1b} and James A. Nusz

Contribution from the William A. Noyes Laboratory, University of Illinois, Urbana, Illinois 61801, and from the R. B. Wetherill Laboratory, Purdue University, West Lafayette, Indiana 47907. Received May 22, 1975

Abstract: Further studies of the enthalpies of adduct formation of bis(hexafluoroacetylacetonato)copper(II) with a series of Lewis bases revealed several exceptions to our reported E and C correlations. Depending on the base, different structural isomers are formed, and this effect was investigated to ascertain if it was the source of the discrepancy. The type of isomer formed with xylene as solvent was determined from an analysis of the ligand hyperfine structure in the EPR spectrum of the adduct. Hexafluoroacetylacetonate, which had been isotopically enriched with ^{17}O nuclei ($I = 5/2$), was used to infer the structure of adducts of oxygen and sulfur donors. In every case, the adducts were found to be square pyramidal. All of the oxygen donors that were examined as well as acetonitrile and the predominant isomer of the tetrahydrothiophene adduct were found to involve axial coordination of the added base, whereas pyridine, quinuclidine, and triphenylphosphine and a small percentage of the tetrahydrothiophene adduct were found to involve basal coordination of the added base. A refined set of E_A and C_A values are reported for this acid, and the same E_A and C_A numbers were found to predict the enthalpy of adduct formation irrespective of the isomer which is formed. A possible explanation for the exceptions to the E and C fit is offered which rationalizes the weaker than expected bond strengths of third-row donors.

In an earlier study, thermodynamic data for the formation of 1:1 adducts of bis(hexafluoroacetylacetonato)copper(II), $\text{Cu}(\text{hfac})_2$, with various Lewis bases were investigated.^{2a} Values were reported for E_A and C_A which when substituted into eq 1 with the appropriate E_B and C_B values for the bases^{2b} reproduced the enthalpy of adduct formation within experimental error.

$$-\Delta H = E_A E_B + C_A C_B \quad (1)$$

Further refinement of the parameters³ also led to an excellent fit of the data employing $C_A = 1.40 \pm 0.13$ and $E_A = 3.39 \pm 0.36$. For the base triethylamine, the calculated enthalpy was some 3 kcal mole⁻¹ higher than the observed value. This discrepancy was dismissed in view of the known encounter of steric problems with this donor. However, in the course of carrying out additional studies, we found other systems which did not obey eq 1, but in which steric complications were not expected. One possible rationalization of this problem supposes the formation of different isomers or mixtures of isomers in solution when the base is varied; i.e., the group of oxygen donors (which fit the E and C equation) could form adducts with the base apical, but other donors would form some or all of an isomer in which the donor occupies a basal position, vide infra. The basal isomer adduct could require a different set of E_A and C_A parameters than the apical adducts.

Evidence for the basal coordination of pyridine in a square-pyramidal complex of $\text{Cu}(\text{hfac})_2$ has been reported by Wayland and co-workers.⁴ A more recent report from that laboratory shows that, depending upon solvent, basal or apical adducts with triphenylphosphine may be obtained.⁵

The extension of eq 1 to transition metal systems is important for the bond types are considerably more complicated in transition metal complexes than the majority of the systems involved in the E and C correlation. Discovery of systems which do not obey the E and C equation and their systematic investigation may suggest important effects that contribute to bonding interactions in this area. Accordingly, it is critical to ascertain, if possible, what causes the complications in the $\text{Cu}(\text{hfac})_2$ systems. Here we report some further thermodynamic data for this acid and an extensive spectroscopic investigation of adducts of this acid in an attempt to elucidate the geometries in solution. Our spectroscopic work includes an

analysis of the ESR spectrum of O^{17} enriched $\text{Cu}(\text{hfac})_2$ and several adducts.

Experimental Section

Materials. All solvents used were reagent grade. The carbon tetrachloride, cyclohexane, and *n*-hexane were dried over Linde 4A molecular sieves at least 24 h. Methylene chloride was distilled from CaCl_2 and xylene was distilled from P_4O_{10} after stirring with concentrated H_2SO_4 and then washing with water.

Tetrahydrothiophene, THTP, was distilled from CaH_2 under reduced pressure while 1-phospha-4-ethyl-2,6,7-trioxo[2.2.2]bicyclooctane, (caged phosphite), 1-aza[2.2.2]bicyclooctane (quinuclidine), and trimethylphosphine oxide were purified by sublimation. Pyridine and 4-methylpyridine were distilled from barium oxide. 1-Methylimidazole and hexamethylphosphoramide were purified by distillation, the latter at reduced pressure.

Peninsular Chemresearch bis(hexafluoroacetylacetonato)copper(II), $(\text{Cu}(\text{hfac})_2)$, or synthetically prepared, vide infra, $\text{Cu}(\text{hfac})_2$ was sublimed several times at 90 °C (1 mm.) and stored over P_4O_{10} in a desiccator. Isotopically pure ^{63}CuO (99.7%) was obtained from Oak Ridge National Laboratory and ^{17}O enriched (44%) water was obtained from Los Alamos National Laboratory. The best preparation of enriched $\text{Cu}(\text{hfac})_2$ was done as follows. First, 34.2 mg of ^{63}CuO was dissolved in 1 M HCl and then dried by evaporation and then under vacuo over P_4O_{10} and a dish of KOH. A solution of 5.2 g of NaOH in 15.6 g of H_2O (distilled water) was prepared and cooled to 0 °C. Then, 60 μl of the NaOH solution was added to 75 μl of the labeled water. Next this solution was added to 0.82 mmol (0.170 g) of hexafluoroacetylacetonate and the resulting solution was stirred ~6 h in a 5-ml volumetric flask. Then the anhydrous $^{63}\text{CuCl}_2$ was added, followed by 4 ml of CH_2Cl_2 and stirring. After about 2 h the CH_2Cl_2 was evaporated under a stream of N_2 and the $\text{Cu}(\text{hfac})_2$ first claimed and then purified by sublimation.

Apparatus and Procedure. The calorimeter has been described.⁶ At all times care was taken to ensure that the $\text{Cu}(\text{hfac})_2$ solutions were rigorously dry. The volumetric flasks were dried in an oven and allowed to cool in a large desiccator over P_4O_{10} . After weighing, they were charged with $\text{Cu}(\text{hfac})_2$ in a glove bag under an atmosphere of dry N_2 and then stored overnight in a desiccator over P_4O_{10} and under vacuo. Then, a second weighing gave the amount of $\text{Cu}(\text{hfac})_2$ present and finally the dry solvent was added in a glove bag. Serum stoppers were used to seal the flasks. The total base concentration never exceeded the total concentration of $\text{Cu}(\text{hfac})_2$ during a run. The reliability of the thermodynamic results was checked in each case by inspecting the K^{-1} vs. ΔH plots to ensure the data points gave rise to lines having significantly different slopes.

Table I. Enthalpies and Equilibrium Constants for 1:1 Adduct Formation of Cu(hfac)₂

Base	Solvent	<i>K</i>	$-\Delta H_{\text{meas}}^a$	σ_m^b/σ_c	$-\Delta H_{\text{corr}}^{a,c}$	$-\Delta H_{\text{calcd}}^{a,d}$
(CH ₃) ₃ PO	CCl ₄	3(±0.4) × 10 ³	11.6 ± 1.2	5.3		11.7
[(CH ₃) ₂ N] ₃ PO	CCl ₄	1(±0.4) × 10 ⁴	10.1 ± 0.4	1.4		10.1
CH ₃ C(O)N(CH ₃) ₂	CCl ₄	1.7(±0.4) × 10 ³	8.0 ± 0.2	<i>e</i>		8.1
CH ₃ COOC ₂ H ₅	<i>o</i> -Cl ₂ C ₆ H ₄	<i>h</i>	6.6 ± 0.2	<i>e</i>		
	CCl ₄	1.9(±0.4) × 10 ²	5.9 ± 0.3	<i>e</i>		5.7
(CH ₃) ₂ SO	CCl ₄	<i>h</i>	8.5 ± 0.3	<i>e</i>		8.5
(CH ₂) ₄ O	<i>o</i> -Cl ₂ C ₆ H ₄	3.5(±0.5) × 10 ³	7.2 ± 0.2	<i>e</i>	8.6	8.5
(CH ₂) ₄ O	CCl ₄		9.1	<i>e</i>		8.2
C ₉ H ₁₈ NO	C ₆ H ₁₂	4.2(±1.9) × 10 ³	11.7 ⁱ	<i>e</i>		11.6
C ₆ H ₁₀ O	CCl ₄		8.8	<i>e</i>		8.7
Caged phosphite	CCl ₄	52	6.5	<i>e</i>		10.6
(CH ₃ O) ₃ P	<i>o</i> -Cl ₂ C ₆ H ₄	4.2(±0.2) × 10 ²	5.5 ± 0.1	2.8	6.9	11.7
(CH ₃ O) ₃ P	CH ₂ Cl ₂	2.6(±0.1) × 10 ²	6.0 ± 0.1	5.4	7.0	11.7
(CH ₂) ₄ S	CCl ₄	1.8(±0.4) × 10 ²	6.9 ± 0.3	2.6	7.9	11.9
(CH ₂) ₄ S	CH ₂ Cl ₂	79 ± 5	4.7 ± 0.1	7.7	5.3	11.9
(CH ₂) ₄ S	<i>o</i> -Cl ₂ C ₆ H ₄	99 ± 5	4.6 ± 0.1	6.2		11.9
C ₅ H ₅ N	C ₆ H ₁₂	<i>h</i>	13.8 ^g	<i>e</i>		12.8
C ₅ H ₅ N	CH ₂ Cl ₂	3.4(±0.9) × 10 ⁴	10.6 ± 0.2	1.7	12.6	12.8
C ₅ H ₅ N	CCl ₄		11.8	<i>e</i>	<i>f</i>	12.8
Quinuclidine	C ₆ H ₁₂	4.1(±0.6) × 10 ³	19.7 ± 0.2	2.4		20.4
MeIm	CCl ₄	10 ⁷	15.5 ± 0.4	1.1		15.4

^a In units of kcal mol⁻¹. ^b Ratio of the marginal standard deviation in ΔH to the conditional standard deviation. See ref 12. ^c Solvent-corrected enthalpy. ^d Enthalpy calculated using $-\Delta H = E_A E_B + C_A C_B$ where $E_A = 3.46 \pm 0.06$, $C_A = 1.36 \pm 0.02$. ^e Obtained from earlier work of this laboratory. See ref 2. ^f R. S. Drago et al., *J. Am. Chem. Soc.*, **96**, 2083 (1974). ^g Due to limited solubility of this adduct in cyclohexane, only the first base injection could be utilized and the data are not reliable. ^h *K* could not be measured. See ref 21. ⁱ Y. Y. Lim and R. S. Drago, *Inorg. Chem.*, **11**, 1334 (1972).

A Varian XL-100 was used for attempts to observe ¹³C NMR. Overnight runs were made with a net accumulation of over 12 000 transients. Broadline ¹⁹F NMR experiments were performed on a Varian Q band instrument using solid samples. The mass spectral measurements were obtained with a CH 5 spectrometer. The EPR measurements were performed at X Band with a Varian E9 instrument equipped with a standard temperature control unit. All measurements reported were made at liquid nitrogen temperature with a modulation amplitude of about 1 G. The EPR tubes were filled in a dry box with a nitrogen atmosphere and sealed off under vacuum at the Pyrex side of a graded seal with the sample on the quartz side. The concentration of copper was 44 mM for the free acid run and about 8 mM for the adduct solutions. In all instances, the copper to base stoichiometry was 1:1 in the adduct solutions.

Calculations. The data treatment for the calorimetry results has been described previously.⁷ The best values of *K* and $-\Delta H$ are obtained from a least-squares minimization of the function

$$R = \sum_{\text{obsd}} (H'_{\text{obsd}} - H'_{\text{calcd}})^2$$

where H'_{obsd} is the experimentally observed enthalpy, H'_{calcd} is the enthalpy calculated from the "best-fit" values of *K* and ΔH , and *R* is the least-squares minimization function. Such a procedure is standard.⁸

The mass spectrum was used to determine isotopic enrichment of Cu(hfac)₂. The parent peak region (mass = 477) was selected for the calculation. First, the net intensities in this region for the ¹⁷O, ¹⁸O enriched sample and for the sample without this enrichment were normalized to the same value. The intensities for the samples in this region were stored in the arrays I17 and I18, respectively, where I17(1) contained the intensity of the enriched sample as mass 477 and I17(2) contained the intensity for the peak at mass 478, etc. Let (*n*₁₇, *n*₁₈) denote the fractional abundance of the species containing *n*₁₇ of the ¹⁷O nuclei and *n*₁₈ of the ¹⁸O nuclei. These fractional abundances were computed using the multinomial coefficients

$$(n_{17}, n_{18}) = \frac{4!}{(n_{17})!(n_{18})!(4 - n_{17} - n_{18})!} (P_{17})^{n_{17}} (P_{18})^{n_{18}} (1 - P_{17} - P_{18})^{(4 - n_{17} - n_{18})}$$

where *P*₁₇ is the fractional abundance of ¹⁷O and *P*₁₈ is the fractional abundance of ¹⁸O. The calculated mass spectrum for the enriched sample was stored in the array CALC and a given peak was calculated as

$$\begin{aligned} \text{CALC}(K) = & \text{INO}(K) - (1,0)*\text{INO}(K) - (2,0)*\text{INO}(K) \dots \\ & - (0,4)*\text{INO}(K) + (1,0)*\text{INO}(K - 1) \\ & + (2,0)*\text{INO}(K - 2) + \dots + (0,4)*\text{INO}(K - 8) \end{aligned}$$

where an asterisk indicates multiplication. A least-squares program SEEK⁹ was used to find the best estimates for *P*₁₇ and *P*₁₈ by minimization of $\sum_K (\text{CALC}(K) - 117(K))^2$.

For the analysis of the EPR spectra, a program which has been described¹⁰ was used. It was assumed that the *g* tensor and the hyperfine coupling tensor to ⁶³Cu had the same principal axis system. The calculation was performed once including isotropic ¹⁷O hyperfine coupling and once without and then these two were summed and compared with the experimental spectra. By varying the proportion of the two calculations in the summed spectrum, in principle, one can obtain the fraction showing an ¹⁷O hyperfine interaction.

Results

The calorimetric data were analyzed assuming 1:1 adduct formation and good agreement between the calculated and observed H' values was found in each case. In Table I, the enthalpy and formation constant obtained for each base are listed as well as the solvent used and the enthalpy predicted by eq 1; vide infra. For convenience, experimental results from previous studies are summarized.

Using the known *E*_B and *C*_B parameters for each base^{2b} and eq 1, the best estimates of the *E*_A and *C*_A parameters for Cu(hfac)₂ were found to be *E*_A = 3.46 and *C*_A = 1.36. The enthalpy data for THTP and caged phosphite were not used in this analysis. As has been described previously,⁷ the reliability of the *E* and *C* fit to enthalpy data can be discerned from a graphical presentation of the data. The graph is presented in Figure 1.

Several methods were employed in an effort to obtain information about the structure of the adducts in solution. In the interval from 600 to 2000 cm⁻¹, we could find little change in the solution infrared spectrum of Cu(hfac)₂ upon adduct formation. We also examined the EPR of frozen solutions of the free acid and various of its adducts. The parallel region was analyzed in each case and the perpendicular region was analyzed in some cases. In Table II the spin Hamiltonian parameters which were found are reported.

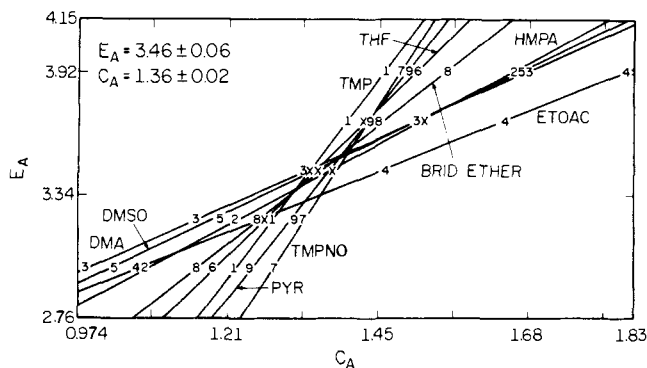


Figure 1. E_A vs. C_A for $\text{Cu}(\text{hfac})_2$.

Table II. EPR Parameters

Base	g_z	A_z , cm^{-1}	g_x	A_x , cm^{-1}	g_y	A_y , cm^{-1}
	2.290	0.0176	2.061	0.0017	2.063	0.0017
DMA	2.335	0.0149	2.073	~0.0005	2.074	~0.0005
H_2O	2.321	0.0160	2.069	~0.0003	2.070	~0.0003
HMPA	2.350	0.0144				
THF	2.326	0.0158				
Pyr	2.310	0.0162				
CH_3CN	2.325	0.0155	2.064		2.065	
PPh_3	2.257	0.0157				
THTP ^a	2.325	0.0155				
THTP ^b	2.284	0.0162				

^a Axial adduct. ^b Basal adduct.

Table III. Mass Spectrum Intensities

Peak	(63,16) ^a	(63,17) ^a	(63,17) ^b
P	16.063	16.43	16.39
P + 1	1.938	10.09	10.05
P + 2	0.320	8.13	8.11
P + 3	0.028	3.12	3.10
P + 4		1.33	1.29
P + 5		0.31	0.33
P + 6		0.08	0.09

^a Experimental. ^b Calculated.

Finally, we measured frozen solution EPR spectra of the free acid and several adducts which contain ^{17}O enriched hfac. These samples were prepared from isotopically enriched ^{63}Cu as well. By the method described in the Experimental Section, the net fractional abundances of ^{17}O and ^{18}O were found to be 0.102 and 0.067, respectively. The ratio of these values is 1.53, which is in good agreement with the $^{17}\text{O}/^{18}\text{O}$ abundance ratio of 1.57 quoted for the enriched H_2O solution. The fit of the mass spectrum intensities is presented in Table III. Thus, our enriched sample contained about 30% of its molecules having a single ^{17}O nucleus and about 5% having two ^{17}O nuclei.

The EPR spectrum of frozen solutions containing the enriched compound showed additional fine structure because of hyperfine coupling to the ^{17}O nucleus which has a spin of $I = 5/2$. In Figure 2, the EPR spectrum of a frozen solution of the free acid is presented as well as the computer simulation from which the parameters in Table II were derived. In principle, the intensity data would determine how many equivalent hfac oxygens are present in the adducts. Thus, if all four oxygens are equivalent, 30% of the net intensity should show hyperfine splitting to an ^{17}O nucleus and 70% should not. (In this approximation, the small fraction of molecules containing two

^{17}O nuclei is ignored.) The spectra of the fractions with and without ^{17}O hyperfine structure should be identical in all other respects such as g values, line shapes, etc. If three equivalent oxygens were present in an adduct and the fourth had a negligible hyperfine interaction, *vide infra*, the relevant percentages are 25% with ^{17}O hyperfine splitting and 75% without. Unfortunately, this kind of quantitative analysis was not possible because we were unable to fit the observed line shapes with sufficient accuracy for the quantitative comparison. Neither Gaussian nor Lorentzian line shapes have a good enough fit. In Figure 3, the low field, or parallel region, is presented for three of the adducts. It is seen that the hyperfine coupling to ^{17}O is clearly resolved in the peak at lowest magnetic field strength for both the oxygen and the sulfur donor. The only ligand hyperfine which is resolved for the pyridine adduct is the coupling to the ^{14}N nucleus which has a nuclear spin $I = 1$.

Figure 4 shows the low field region for the EPR spectrum of a 1:1 solution of THTP and $\text{Cu}(\text{hfac})_2$. The predominant features of the spectrum are assigned to the 1:1 axial adduct while a small percentage is assigned to the 1:1 basal adduct of THTP with $\text{Cu}(\text{hfac})_2$.

Discussion

The results obtained from our calorimetric studies are summarized in Table I. The raw data are available in the microfilm edition.¹¹ In addition to the enthalpies, we have reported the ratio of the marginal to conditional standard deviation in the table. As described earlier,¹² these ratios are offered in place of the K^{-1} vs. ΔH plots described in our previous work.

Our experience leads us to believe that the most reliable results are associated with both a small conditional standard deviation as well as a small ratio of the marginal standard deviation to the conditional standard deviation. Attempts to quantify these requirements have been presented¹² and they generally ensure that reliable K^{-1} vs. ΔH plots are obtained; that is, the data points define a set of curves that have a small region of intersection and the curves have a significant variation of slopes in that region. The ratios reported in Table I indicate a good definition of the two variables in most of the experiments reported here.

As can be seen from the data in Table I, excellent agreement is found between the enthalpy values predicted by eq 1 and those measured experimentally for most of the donors studied. Pyridine forms an adduct whose limited solubility in cyclohexane hampered an accurate measurement. The enthalpy reported in Table I was that obtained by employing data only from the first base injection and some solid adduct may have formed so even this result could have an enthalpy contribution from lattice energy. In order to overcome this problem, the adduct formation reaction was studied in CH_2Cl_2 and *o*-dichlorobenzene as solvents and corrected using reported procedures.^{13,14} The fact that the data in two solvents as different as CH_2Cl_2 and *o*- $\text{Cl}_2\text{C}_6\text{H}_4$ correct back to about the same value ($12.8 \text{ kcal mol}^{-1}$) leads us to believe that the result from these studies is the correct solvent minimized enthalpy and that there are complications from colloidal suspension of a solid resulting in the (higher) value obtained from cyclohexane.

The results obtained with the donors $(-\text{CH}_2\text{CH}_2)_2\text{S}$, $(\text{CH}_3\text{O})_3\text{P}$, and $\text{C}_2\text{H}_5-\text{C}(\text{CH}_2\text{O})_3\text{P}$ are not predicted by eq 1. Accordingly, the reported set of E_A and C_A values were calculated from the data in Table I excluding these donors. The new values reported here ($E_A = 3.46 \pm 0.06$, $C_A = 1.36 \pm 0.02$) are refined considerably over those reported earlier ($E_A = 3.39 \pm 0.36$, $C_A = 1.40 \pm 0.13$) as indicated by the reduced error limits. A series of bases was used which involved a wide range of C_B/E_B values in this study. As discussed elsewhere⁷

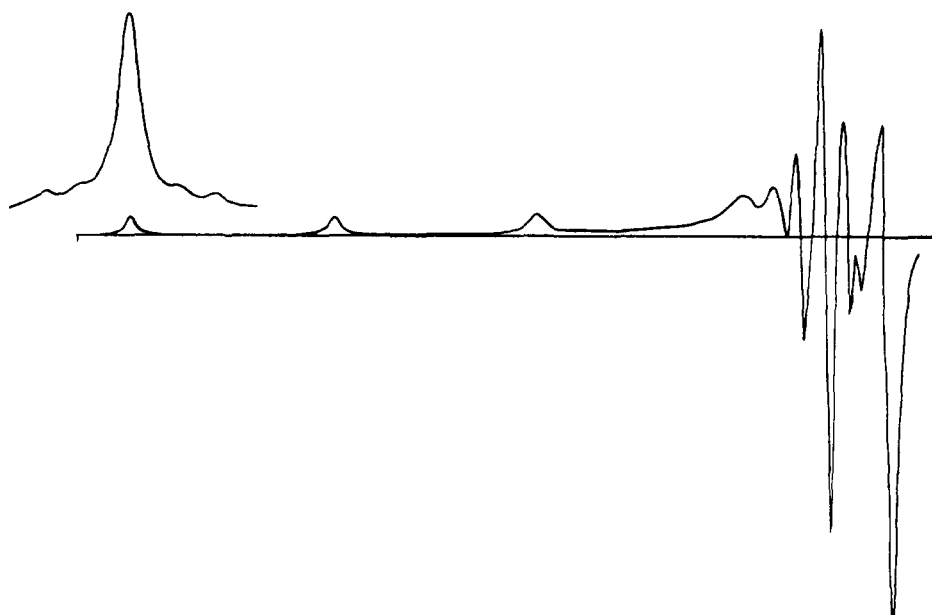


Figure 2. The simulated EPR spectrum of free $\text{Cu}(\text{hfac})_2$ is displayed below the experimental spectrum. The lowest field feature in the experimental spectrum is presented in an expanded scale. The spin Hamiltonian parameters for the simulated spectrum are those from Table II.

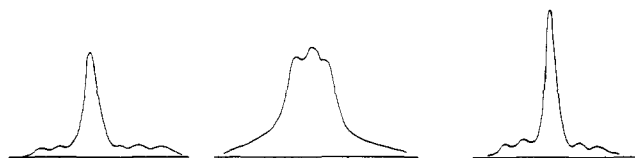


Figure 3. The traces are for the lowest field feature from the spectra of 1:1 adducts of $\text{Cu}(\text{hfac})_2$ with THTP, pyridine, and DMA (left to right). The tick marks represent a spacing of 40 G in each case. For pyridine only ^{14}N hyperfine splitting is resolved, while THTP and DMA show ^{17}O hyperfine splitting.

this is essential to ensure that the E and C parameters obtained are reliable.

The donor $(-\text{CH}_2\text{CH}_2-)_2\text{S}$ was investigated in several solvents to ascertain if the medium could be the cause of the problem. A value of $0.6 \text{ kcal mol}^{-1}$ is the predicted¹³ correction for the CH_2Cl_2 result leading to a corrected enthalpy of $-5.3 \text{ kcal mol}^{-1}$. Thus, not only do these systems not obey the E and C equation, but, as we have reported, they also cause a

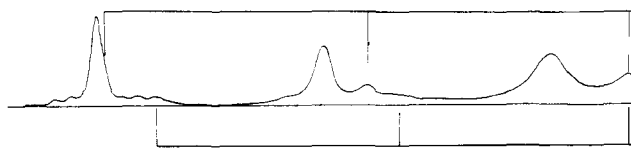


Figure 4. A trace of the low field region of the spectrum of a 1:1 solution of THTP and $\text{Cu}(\text{hfac})_2$. The main features are assigned to the spectrum of the 1:1 adduct with axial coordination. The markers above the baseline indicate contributions assigned to uncomplexed $\text{Cu}(\text{hfac})_2$. The markers below the baseline indicate contributions assigned to the 1:1 basal adduct of THTP with $\text{Cu}(\text{hfac})_2$.

breakdown in the solvent correction procedures which have worked so well in the past. The cause of the solvent correction failure with this donor is unknown. However, this could possibly be due to the fact that the enthalpy measured in CH_2Cl_2 is not well defined as shown by its relatively large ratio of marginal to conditional standard deviations.

The phosphorus donor $(\text{CH}_3\text{O})_3\text{P}$ was also investigated in solvents which have the potential of undergoing a specific in-

teraction with the phosphorus and confusing the interpretation of the resulting thermodynamic data. The CH_2Cl_2 solvent corrected enthalpy with the donor $(\text{CH}_3\text{O})_3\text{P}$ is -7.0 kcal mol^{-1} . The reported¹⁵ value for the correction in *o*- $\text{Cl}_2\text{C}_6\text{H}_4$ produces a value of 6.9 kcal mol^{-1} . Thus, we are confident of the solvent-minimized value of the enthalpy for the adduct with $(\text{CH}_3\text{O})_3\text{P}$.

The sulfur and phosphorus donor have enthalpies of adduct formation well below those predicted by the E and C equation. The sulfur donors used have been studied extensively in previous work and the E_B and C_B numbers are well defined. Exceptions to eq 1 are of interest since they may provide insight about additional factors which influence bond strengths in adducts. One possible explanation for this discrepancy is that different isomers may form with different bases which require different E_A and C_A numbers. Since the enthalpies are so much lower than predicted for these systems, this explanation is reasonable only if there is some entropic reason to provide the driving force for coordination to this lower enthalpy site. To test this hypothesis, we undertook studies to ascertain the structures of different adducts which are formed.

Structural Studies of the Adducts. The two limiting structures expected for the five-coordinate adducts of $\text{Cu}(\text{hfac})_2$ are a trigonal bipyramid and a square pyramid. In general, trigonal-bipyramidal complexes of copper exhibit d_{z^2} ground states¹⁶ which have $g_{x,y} \approx 2.2$. In the adducts we studied $g_z \approx 2.3$ and $g_{x,y} \approx 2.07$ which are typical values for square-pyramidal complexes with a $d_{x^2-y^2}$ ground state.¹⁷ Thus, in all cases, the 1:1 adducts of $\text{Cu}(\text{hfac})_2$ with the bases we have employed assume a square-pyramidal structure. In C_{2v} symmetry, if ligand covalency effects are ignored, the expression for g_z is given by¹⁶

$$g_z = 2.0023 - \frac{8\lambda \cos^2 \alpha}{(E_{xy} - E_{x^2-y^2})}$$

where $\lambda = -828$ cm^{-1} is the spin-orbit coupling constant, E_{xy} and $E_{x^2-y^2}$ denote the energy of the d_{xy} and $d_{x^2-y^2}$ orbitals, respectively, and $\cos \alpha$ is the coefficient of $d_{x^2-y^2}$ in the ground state. Some d_{z^2} character is also allowed to mix into the orbital containing the unpaired electron in the ground state in this symmetry. In most cases upon adduct formation g_z increases over the value in the free acid spectrum and this probably reflects a decreased separation between d_{xy} and $d_{x^2-y^2}$ for the adducts. There are two isomers of the limiting square-pyramidal structure. One involves apical coordination of the Lewis base and one involves basal coordination. Wayland has proposed that the basal structure is obtained with pyridine,⁴ because ^{14}N ligand hyperfine structure appeared in the frozen solution EPR spectrum. If the pyridine coordinated in the apical position, then the sp^2 donor orbital on nitrogen would be directed along the z axis, orthogonal to $d_{x^2-y^2}$, which contains the unpaired spin. In that event, the spin density on nitrogen should be small and no resolved ^{14}N hyperfine splitting would be expected.^{4,18}

Though the ligand hyperfine effect is a useful probe of the adduct structure, its use is limited to bases, e.g., nitrogen and phosphorus, whose donor atoms have a nucleus of nonzero spin. If bases with natural abundance isotopes are used, this experiment does not provide information on the geometry of oxygen and sulfur donors.

In order to obtain structural information about the adducts in solution which are reported in Table I, a variety of physical methods were considered. The structures of copper(II) complexes are notoriously difficult to determine in solution because the electronic spectrum, ESR, and magnetism are all relatively insensitive to geometry.

To overcome these limitations we enriched the hfac oxygens with ^{17}O ($I = 5/2$) in order to use the ligand hyperfine probe. For the apical adducts of the ^{17}O -enriched $\text{Cu}(\text{hfac})_2$, we ex-

pected to observe hyperfine structure from four essentially equivalent oxygens, whereas the basal adduct would have lower symmetry. In the latter case the ^{17}O hyperfine coupling constants would be different for the nonequivalent oxygens and would give rise to a broadened, poorly resolved ^{17}O hyperfine envelope.

The frozen solution EPR spectra of the free acid and the 1:1 adducts of oxygen donors showed well resolved ^{17}O hyperfine structure in the lowest field feature of the ^{63}Cu hyperfine structure in the g_z region. This structure was also found in the spectrum of the predominant species in the spectrum of a 1:1 mixture of $\text{Cu}(\text{hfac})_2$ and THTP as well as in the spectrum of the 1:1 complex with CH_3CN . Because the line shapes could not be simulated with sufficient accuracy, quantitative analysis of the intensities could not be made. However, for the reasons described above, the excellent resolution of the ^{17}O splitting which is observed for these systems would not be expected for a basal adduct and argues strongly for apical coordination. In this regard, it should be noted that no ^{17}O splitting could be resolved in the case of pyridine, quinuclidine, or triphenylphosphine. In general, the EPR spectra of the latter systems had appreciably broader lines than the spectra for the oxygen donor adducts.¹⁹

The experiments involving ^{17}O enrichment show that the oxygen bases coordinate in the apical position. For the pyridine and triphenylphosphine adducts no ^{17}O splitting was resolved, but splitting from ^{14}N and ^{31}P , respectively, was observed. These results are consistent with basal coordination.⁴ So far, however, we have ignored the fact that in C_{2v} symmetry and lower d_{z^2} can mix with $d_{x^2-y^2}$. Since the donor orbital of a base coordinated in the apical position can interact with d_{z^2} , this overlap would lead to unpaired spin density on the donor atom. However, as described next, the data suggest that the d_{z^2} admixture is small, and lead to the conclusion that the ^{14}N and ^{31}P hyperfine splittings are associated with basal coordination.

We have already noted that the g values are consistent with a $d_{x^2-y^2}$ ground state. Furthermore, we note that the magnitude of the ^{14}N coupling constant for the pyridine $\text{Cu}(\text{hfac})_2$ adduct is ~ 9 G^4 and is typical of that for an inplane nitrogen,¹⁸ whereas the ^{14}N coupling constant for the pyridine adduct of $\text{Cu}(\text{acac})_2$ is only 0.7 G^4 . Presumably, the latter complex involves an apical coordination of pyridine. Additional evidence comes from the studies involving CH_3CN . In the adduct with CH_3CN , we found well resolved ^{17}O hyperfine structure and line widths comparable to those observed for the adducts of the oxygen donors which imply the CH_3CN binds apically. However, we did not observe ^{14}N hyperfine splitting in the spectrum. If the d_{z^2} admixture were appreciable, we should have resolved hyperfine coupling to the nitrogen of CH_3CN . To see this consider the principal contributions to the ligand hyperfine coupling:²⁰ (i) delocalization of unpaired spin density into the valence orbital of the ligand (we are ignoring polarization of the ligand core orbitals which gives a contribution that is opposite in sign to the contribution from the valence s orbital, since it should be a small correction²¹), (ii) dipolar coupling of the ligand nucleus to unpaired spin density in the valence p orbitals of the ligand, and (iii) dipolar coupling of the ligand nucleus to unpaired spin density over the rest of the molecule. The first interaction is the isotropic Fermi contact interaction while the second two comprise the anisotropic dipolar interaction which is averaged over the spatial distribution of unpaired spin. Now, the donor orbital of the pyridine is approximately an sp^2 hybrid orbital at the nitrogen while that of CH_3CN is approximately an sp hybrid orbital. Thus, all else the same, one would expect a larger ^{14}N coupling in CH_3CN than in pyridine because the Fermi contact interaction will be larger in the former which has a greater fraction of s orbital character involved in the bonding lone pair. Even with lesser covalency in the acetonitrile adduct, we expect that the en-

hanced s character in the donor orbital should have led to a detectable nitrogen hyperfine if there were appreciable spin in d_{z^2} . The conclusion is unchanged if we include the dipolar contribution from the unpaired spin averaged over the ligand p orbital, because the dipolar contribution would have the same sign as the Fermi contact contribution in the g_z region and would enhance the splitting. The dipolar interaction of the ligand nuclear spin with the unpaired spin averaged over the metal orbitals is negligible since the ligand nucleus is about 0.2 nm separated from the metal nucleus and the dipolar interaction decreases with the inverse third power of the distance. We conclude the d_{z^2} admixture is small and quinuclidine must also bind $\text{Cu}(\text{hfac})_2$ in basal position with the donor orbital overlapping the $d_{x^2-y^2}$ orbital. Similar considerations apply for triphenylphosphine and the analysis of the hyperfine tensor components which is described next provides additional evidence for the basal coordination of the phosphine donor.

In general for apical adducts the ligand hyperfine coupling constant in the g_z region is expected to be larger than the isotropic interaction, which is measured in fluid solution. Similarly, in the high field region, it will be smaller than the isotropic interaction.²² For the PPh_3 adduct, Zelonka and Baird have shown that the isotropic hyperfine coupling to ^{31}P is 132 G.²³ In frozen solution, we find a ^{31}P coupling constant of 123 G in the g_z region and a larger constant of 158 G involved in the $g_{x,y}$ region.²⁴ These results are inconsistent with axial coordination of the ^{31}P and imply basal coordination.

It is noteworthy that g_z for the triphenylphosphine adduct is much smaller than that of the other adducts, including pyridine which also binds basally. As discussed by Wayland,⁵ it probably is due to a strong covalent interaction with phosphorus. This explanation would predict that a basal adduct of THTP should have an anomalously low value for g_z as well. Examination of the low field region of the THTP adduct shown in Figure 4 reveals a four-line pattern which we assign to the apical adduct and lines due to uncomplexed $\text{Cu}(\text{hfac})_2$. In addition, two additional weak features are resolved. Based on the discussion above, we assign these to be the two low field components of the spectrum of the basal adduct with $g_z = 2.284$. The other two components are obscured by overlap with the more intense lines due to the free acid and with the $g_{x,y}$ features. Thus, in xylene, it appears that a mixture of isomers is obtained with THTP.

In summary, the EPR results confirm that both apical and basal adducts are formed with $\text{Cu}(\text{hfac})_2$. We find that pyridine, quinuclidine, PPh_3 , and a small percentage of the THTP system go basally while the others bind apically in xylene.

Isomerism and the E and C Predictions. An important contribution of the E and C equation to the systematization of inorganic chemistry is based on its ability to predict the enthalpy for a normal interaction of a Lewis base with a Lewis acid, e.g., an oxygen donor with $\text{Cu}(\text{hfac})_2$ to form an apical adduct. Since hundreds of adducts obey the E and C equation, normal is defined pragmatically as those that conform. In this context, it is significant that the enthalpy predicted for the apical adduct of pyridine is that measured experimentally for the basal adduct. Close agreement is also found for quinuclidine. This implies that for $\text{Cu}(\text{hfac})_2$ the E_A and C_A numbers for the acid reacting to form a basal isomers are comparable to the parameters for the apical isomer. Thus, the isomer that results is largely determined by entropic considerations. This conclusion could not have been drawn if we were not able to predict the enthalpy of the apical adduct with the E and C equation. The similarity in the acidity of the two sites is consistent with the recent report of Wayland et al.⁵ Comparable free energies of formation of the two isomers are indicated because minor variation in the solvent interconverts basal and apical phosphine adducts.

If the two acid sites have similar E_A and C_A values, we

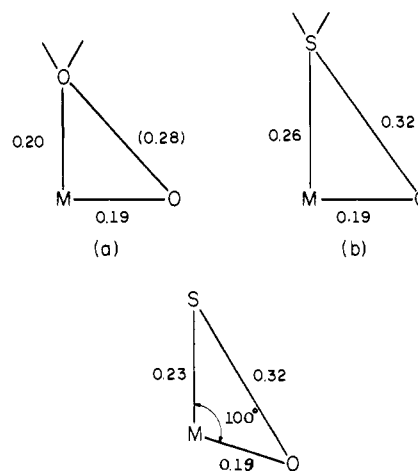


Figure 5. Models for the hard sphere calculations. See the text for an explanation of the bond distances shown.

cannot rationalize the discrepancy between the calculated and observed enthalpies for the sulfur and phosphorus donors in terms of isomerism. These systems as well as the BF_3 adducts of phosphorus and sulfur donors are similar in that the measured enthalpies for both acids are considerably lower than predicted. We previously^{2b} labeled these BF_3 adducts as exceptions to our correlation which we did not understand and pointed out that only by finding more exceptions will patterns develop which will enable us to pinpoint the abnormalities. We are now in a position to suggest a rationalization for these discrepancies which will enable us to predict when we can expect exceptions. Boron trifluoride and $\text{Cu}(\text{hfac})_2$ both have relatively small acid centers (the ionic radius for copper²⁵ is 0.092 nm and the covalent radius for boron²⁶ is ~ 0.09 nm) which are flanked by atoms with a large formal negative charge. There is a considerable amount of electron density on these atoms which points toward the incoming ligands. In the case of BF_3 , there is considerable electron density in the B-F π bond. When the incoming ligand is a Lewis base with a large donor atom, the diffuse electron density in the donor orbital of this atom can undergo significantly larger repulsive interaction with this neighboring electron density than the donor orbital of a first-row atom does. Thus, if the E_A and C_A values are parameterized using first-row donor atoms, they will overestimate the enthalpy for a large second-row donor atom because this flanking atom charge repulsion will not be included.

This idea receives support from a crude hard sphere calculation which shows the greater proximity of the sulfur and phosphorus ligands to this neighbor atom charge. In Figure 5a, we see that a typical²⁷ copper–oxygen (of the hfac) distance and sum of van der Waals radii of oxygen–apical oxygen²⁸ permits a copper–apical ligand donor atom distance of 0.204 nm. Bushnell reports typical distances²⁹ for apical oxygen atoms in five-coordinate complexes as 0.22 to 0.24 nm. Belford reports a zinc–ethanol oxygen distance of 0.21 nm in bis-(benzoylacetonato)zinc monoethanolate.³⁰ In contrast to this when the van der Waals radii²⁸ for an apical sulfur donor is used, metal–sulfur donor atom distances of 0.26 nm (Figure 5b) or less will undergo van der Waals contact with the oxygen. The sum of the phosphorus–oxygen van der Waals radii of 0.30 nm is even larger than sulfur–oxygen. There are no data on metal–tetrahydrothiophene bond lengths, but the added 0.03-nm covalent radius of sulfur compared with oxygen would lead to an expected metal–sulfur ligand distance of ~ 0.24 nm in strong sulfur donor adducts. This is well below that for sulfur–oxygen interaction. These calculations are admittedly crude, but they do show that greater repulsions are expected

between the larger donor atoms and the hfac oxygen electron density than in the case of oxygen or nitrogen donor ligands.

These calculations were made employing an O-Cu-S angle of 90°. It is expected that this angle will be greater than 90° in these adducts. In the zinc ethanolate adduct described above, the angle is 100°. This value reduces the metal-sulfur donor atom distance at which van der Waals contacts are expected to 0.23 nm (Figure 5c). The important point is that comparable distortions are expected in the oxygen adduct, so the electrostatic repulsion of the electron density on these atoms with the apical ligand donor atom is expected to be larger for the larger atoms.

The situation is similar in BF₃ where the BF distance is 0.130 nm.²⁵ However, in the case of Al(CH₃)₃ where there are no lone pairs on the CH₃ group and where the formal charge on the methyl group is expected to be considerably less than that on the flanking atoms in Cu(hfac)₂ and BF₃, perfect agreement is found in the predicted and experimental values of the enthalpy for O, N, S, and P donors. It would be of interest to examine the BF₃ and B(CH₃)₃ enthalpies of adduct formation with a series of oxygen, nitrogen, sulfur, and phosphorus donors to ascertain the influence of this neighbor atom repulsive effect. However, there are such limited data on these systems that any parameters one attempts to calculate can be forced to fit the data. We now must conclude that in view of these potential complications, our reported parameters for BF₃ and (CH₃)₃P are highly uncertain.

Another metal complex we have studied is methylcobaloxime, where most of the ligand's negative charge is expected³¹ to be located on the oxime oxygens which are not flanking atoms, but which are well removed from the acidic center. Thus, we find toward methylcobaloxime that O, N, and S donors are all well behaved in terms of the enthalpy predictions by the *E* and *C* equation. The effect we are proposing here is very much like a steric effect and should be treated similarly in the context of the *E* and *C* formulation; i.e., systems in which it is operative should be avoided in empirically obtaining the parameters. The resulting parameters may then be used to predict enthalpies which do not include these repulsive interactions, but which can be used to detect their existence. This type study provides an excellent illustration of the understanding that can result from a quantitative formulation of acid-base interactions.

Acknowledgment. We are indebted to Robert L. Courtright for assisting with calorimetry experiments and thank Professor R. Linn Belford for useful conversations. The mass spectral

data processing equipment employed in this study was provided by NIH Grants CA 11388 and GM 16864, from the National Cancer Institute and the National Institute of General Medicinal Sciences, respectively. The authors gratefully acknowledge the support of this research by the National Science Foundation through Grant NSF GP31431X.

Supplementary Material Available: raw calorimetric data used in obtaining Table I (5 pages). Ordering information is given on any current masthead page.

References and Notes

- (1) (a) Purdue University; (b) University of Illinois.
- (2) (a) W. Partenheimer and R. S. Drago, *Inorg. Chem.*, **9**, 47 (1970); (b) R. S. Drago, *Struct. Bonding (Berlin)*, **15**, 73 (1973).
- (3) R. S. Drago, G. C. Vogel, and T. Needham, *J. Am. Chem. Soc.*, **93**, 6014 (1971).
- (4) B. B. Wayland and M. D. Wisniewski, *Chem. Commun.*, 1025 (1971).
- (5) B. B. Wayland and V. K. Kapur, *Inorg. Chem.*, **13**, 2517 (1974).
- (6) M. S. Nozari and R. S. Drago, *J. Am. Chem. Soc.*, **92**, 7086 (1970).
- (7) (a) T. F. Bolles and R. S. Drago, *J. Am. Chem. Soc.*, **87**, 5015 (1965). (b) The problem has also been formulated for NMR results where *K* and δ , the chemical shift, or *J*, the spin-spin coupling constant, can be determined in the fast exchange region. See F. L. Slejko, R. S. Drago, and G. Brown, *ibid.*, **94**, 9210 (1972), and T. F. Bolles and R. S. Drago, *ibid.*, **88**, 3921 (1966).
- (8) L. G. Sillen, *Acta Chem. Scand.*, **16**, 159 (1962).
- (9) D. R. McMillin, *J. Chem. Educ.*, **51**, 496 (1974).
- (10) A. D. Toy, S. H. H. Chaston, J. R. Pilbrow, and T. D. Smith, *Inorg. Chem.*, **10**, 2219 (1971).
- (11) See paragraph at end of paper regarding supplementary material.
- (12) R. M. Guidry and R. S. Drago, *J. Am. Chem. Soc.*, **95**, 6645 (1973).
- (13) R. S. Drago, J. A. Nusz, and R. C. Courtright, *J. Am. Chem. Soc.*, **96**, 2082 (1974).
- (14) R. S. Drago, M. S. Nozari, and G. C. Vogel, *J. Am. Chem. Soc.*, **94**, 90 (1972).
- (15) M. S. Nozari and R. S. Drago, *Inorg. Chem.*, **11**, 280 (1972).
- (16) B. J. Hathaway and D. E. Billing, *Coord. Chem. Rev.*, **5**, 143 (1970).
- (17) B. B. Wayland and A. F. Garito, *Inorg. Chem.*, **8**, 182 (1969).
- (18) K. E. Falk, E. Ivanova, B. Roos, and T. Vanngard, *Inorg. Chem.*, **9**, 556 (1970).
- (19) A possible source of broadening is hyperfine coupling to protons on the base. We would expect these interactions to be significant only in the basal structure. See Y. Nonaka et al., *Bull. Chem. Soc. Jpn.*, **47**, 312 (1974).
- (20) R. G. Hays, "Electron Spin Resonance of Metal Complexes", T. F. Yen, Ed., Plenum Press, New York, N.Y., 1969, pp 23-32.
- (21) A. Abragam and B. Bleaney, "Electron Paramagnetic Resonance of Transition Ions", Clarendon Press, Oxford, 1970, p 780.
- (22) E. E. Genser, *Inorg. Chem.*, **7**, 13 (1968).
- (23) R. A. Zelonka and M. C. Baird, *Can. J. Chem.*, **50**, 1269 (1972).
- (24) The hyperfine coupling tensor to ³¹P for a basal adduct should be rotated ~90° relative to the *g* tensor axis system.
- (25) F. A. Cotton and G. Wilkinson, "Advanced Inorganic Chemistry", 2nd ed, Wiley, New York, N.Y., 1966, p 45.
- (26) See ref 25, pp 105 and 106.
- (27) P. Jose, S. Ooi, and Q. Fernando, *J. Inorg. Nucl. Chem.*, **39**, 1969 (1971).
- (28) See ref 25, p 115.
- (29) G. W. Bushnell, *Can. J. Chem.*, **49**, 555 (1971).
- (30) R. L. Belford et al., *Inorg. Chem.*, **8**, 1312 (1969).
- (31) R. L. Courtright, R. S. Drago, J. A. Nusz, and M. S. Nozari, *Inorg. Chem.*, **12**, 2809 (1973).